Tectonophysics, 67 (1980) 221—249
Elsevier Scientific Publishing Company, Amsterdam — Printed in The Netherlands

PETROGENESIS OF CATACLASTIC ROCKS WITHIN THE SAN ANDREAS FAULT ZONE OF SOUTHERN CALIFORNIA, U.S.A.

J. LAWFORD ANDERSON [1], ROBERT H. OSBORNE [1] and DONALD F. PALMER [2]

[1] *Department of Geological Sciences, University of Southern California, Los Angeles, CA 90007 (U.S.A.)*
[2] *Department of Geology, Kent State University, Kent, Ohio 44242 (U.S.A.)*

(Received May 23, 1979; revised version accepted August, 1979)

ABSTRACT

Anderson, J.L., Osborne, R.H. and Palmer, D.F., 1980. Petrogenesis of cataclastic rocks within the San Andreas fault zone of southern California, U.S.A. Tectonophysics, 67: 221—249.

This paper petrologically characterizes cataclastic rocks derived from four sites within the San Andreas fault zone of southern California. In this area, the fault traverses an extensive plutonic and metamorphic terrane and the principal cataclastic rock formed at these upper crustal levels is unindurated gouge derived from a range of crystalline rocks including diorite, tonalite, granite, aplite, and pegmatite.

The mineralogical nature of this gouge is decidedly different from the "clay gouge" reported by Wu (1975) for central California and is essentially a rock flour with a quartz, feldspar, biotite, chlorite, amphibole, epidote and oxide mineralogy representing the milled-down equivalent of the original rock. Clay development is minor (less than 4 wt. %) to nonexistent and is exclusively kaolinite. Alterations involve hematitic oxidation, chlorite alteration on biotite and amphibole, and local introduction of calcite. Electron microprobe analysis showed that in general the major minerals were not reequilibrated with the pressure—temperature regime imposed during cataclasis.

Petrochemically, the form of cataclasis that we have investigated is largely an isochemical process. Some hydration occurs but the maximum amount is less than 2.2% added H_2O. Study of a 375 m deep core from a tonalite pluton adjacent to the fault showed that for Si, Al, Ti, Fe, Mg, Mn, K, Na, Li, Rb, and Ba, no leaching and/or enrichment occurred. Several samples experienced a depletion in Sr during cataclasis while lesser number had an enrichment of Ca (result of calcite veining).

Texturally, the fault gouge is not dominated by clay-size material but consists largely of silt and fine sand-sized particles. An intriguing aspect of our work on the drill core is a general decrease in particulate size with depth (and confining pressure) with the predominate shifting sequentially from fine sand to silt-size material.

The original fabric of these rocks is commonly not disrupted during the cataclasis. It is evident that the gouge development in these primarily igneous crystalline terranes is largely an *in situ* process with minimal mixing of rock types. Fabric analyses reveal that brecciation (shattering), not shearing, is the major deformational mechanism at these upper crustal levels.

0040-1951/80/0000—0000/$02.25

INTRODUCTION

Studies leading to earthquake prediction and control require not only a knowledge of the causes and mechanics of earthquakes, but also an understanding of the physical, compositional, and mechanical properties of the geologic system in which they occur. Presently, little has been written about the nature of cataclastic rocks within fault zones except that it is generally markedly different from rocks on either side of the fault; that it may be fault gouge, fault breccia, cataclasite, or mylonite[1]; and that it originates from mechanical crushing of rocks and from varying degrees of secondary chemical and mineralogical alterations by fluids moving through the fault zone (Higgins, 1971). With regard to the gouge typical of upper crustal levels, Wu et al. (1975) note several unknowns: (1) the mineralogy and petrology, (2) the fabric and texture, (3) the quantity and chemistry of pore waters within the fault zone, and (4) the mechanical properties of the fault gouge under the appropriate conditions of temperature, pressure, and solution chemistry.

The importance of cataclastic intrafault material such as fault gouge in controlling the failure characteristics of rocks has been demonstrated in experimental studies. Scholz et al. (1972) noted that the development of gouge allowed the samples to reach a steady-state frictional behavior and that the gouge seems to have the effect of reducing the stress drops to a small fraction of their value for clean ground surfaces. The latter feature concurs with the suggestion by Stesky and Brace (1973) that the presence of low strength alteration materials in the San Andreas fault zone may account for the low frictional shear stress estimates provided from heat flow data relative to the much higher estimates from high-temperature frictional studies.

Wu et al. (1975) have suggested that the mineralogy of gouge may govern the type of failure (creep versus stick-slip) in fault zones. They note that in southern California the San Andreas fault lies mostly within granitic rocks, between Pt. Arena and San Luis Obispo the fault is bordered on the east by Franciscan rocks and on the west by granitic rocks and Cenozoic sedimentary rocks, and that the Hayward and Calaveras faults are within the Franciscan rocks. They argue convincingly that within the fault zone, to a depth of perhaps 12 km, sodic and magnesian-rich Franciscan rocks alter to expandible clay (montmorillonite) gouge which, by its strength, governs the nature of fault movement.

---

[1] Following the nomenclature of Higgins (1971), these cataclastic rocks have the following characteristics: (1) fault breccia- no primary cohesion with more than 30% fragments which are greater than 0.3 mm in diameter, (2) gouge—"paste-like" cataclastic rock with no primary cohesion and less than 30% fragments greater than 0.3 mm, (3) cataclasite—aphanitic cataclastic rock with most fragments less than 0.2 mm and constituting less than 30% and, (4) mylonite-cohesive cataclastic rock with fluxion structure and 10—50% porphyroclasts generally larger than 0.2 mm.

Recent experimental studies, however, have shown that the stabilizing influence of fault gouge decreases with increasing confining pressure. Logan (1977; 1978a, b) has shown that stable sliding is a consequence of low pressure and, even with the presence of fault gouge, the failure characteristics become increasingly unstable and change to a catastrophic stick-slip mode of displacement as the confining pressure is increased. The transition from stable to stick-slip motion is very dependent upon mineralogy. For quartz and feldspar gouge the mechanical transition is at about 2.5 kb. For soft minerals with a high degree of compaction characteristics, such as carbonates, the transition occurs at about 1.0 kb. Although montmorillonite clay gouge certainly enhances stability (transition occurs at about 6.0 kb) other clays, particularly kaolinite, do not readily affect the sliding behavior relative to other gouge mineralogies. Byerlee et al. (1978) have speculated that the overriding factor governing the transition from stable to stick-slip displacement may be the compaction behavior or porosity of the fault gouge. Engelder (1974) has demonstrated that the grain size of cataclastic rocks within fault zones decreases with increasing confining pressure and the resultant loss of porosity (increased compaction) may favor unstable sliding. The prevailing geothermal gradient is also a major factor governing this transition (Brace, 1972) and Logan (1978b) has demonstrated that unstable sliding becomes increasingly stable as temperature increases beyond 400° C.

Unfortunately, there have been few detailed petrologic studies of the cataclastic rocks comprising the intrafault material of fault zones. This is particularly evident for active fault zones, such as the San Andreas, where realistic modeling of rock failure is important. Nason (1972), Wu et al. (1975), Wu (1977), and Wang (1977) have demonstrated the existence of "clay" gouge along the trace of the San Andreas in central California where large sections of the fault exhibit creep slippage (Nason, 1973).

Our work focuses on petrology of cataclastic rocks at four target sites within or marginal to the San Andreas fault zone of southern California (Fig. 1), a region where the present fault is largely "locked". We are concerned with establishing the textural, fabric, mineralogic, and petrochemical nature of the intrafault material. As a preface to the following discussion, our finding confirms that fault gouge is the dominate cataclastic rock type formed at these upper crustal levels rather than fault breccia, cataclasite, or mylonite. The fault trace in southern California traverses an extensive area of crystalline rocks and we have found that gouge derived from parent rocks including diorite, tonalite, aplite and pegmatite has very little clay and is essentially the milled-down "flour" equivalent of the parent rock mineralogy. Moreover, textural analysis reveals a grain size dominated by silt and fine sand particles rather than clay-size material. Hence, this study involves the first documentation of a type of gouge that may characterize intrafault material formed at shallow levels where the fault traverses primarily granitic terranes.

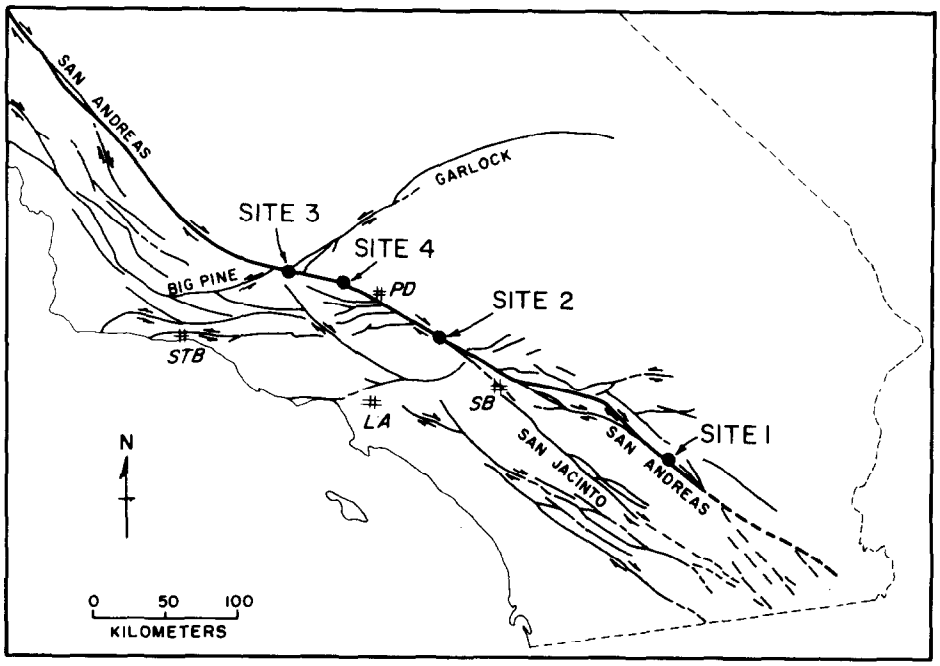

Fig. 1. The San Andreas fault system of southern California showing sample sites 1—4.

DESCRIPTION OF LOCALITIES AND SAMPLES

Site 1 is in the Mecca Hills at the intersection of Painted and Little Painted Canyons where they are crossed by the Painted Canyon fault (Sylvester and Smith, 1975) which defines the northeast margin of the San Andreas fault zone in this area. This fault is not the most active trace but it has excellent exposure of gouge in numerous thrust faults related to compression and uplift of the fault zone. This section in Mecca Hills (Sylvester and Smith, 1975) offers some of the best exposures elucidating the tectonic geometry of the southern San Andreas fault zone. The samples came from gouge zones within numerous faults at this locality and all are within the Precambrian granitic gneiss and migmatite of the Chuckwalla Complex (Miller, 1944).

Site 2 is in the San Andreas fault zone, 1 mile northwest of Big Pines in the San Gabriel Mountains. Here the fault zone is narrow (<0.5 km) and separates granite gneiss from the Pelona schist. Deep erosion along this portion of the fault has exposed fresh samples of fault gouge. Although relict knobs of unaffected protolith are rare, relict textures are evident in most samples and it is possible to collect gouge from a range of crystalline protoliths including granitic gneiss, aplite, and schist. The gouge is cross-cut by thin shear zones (0.25—1.00 cm wide) of highly comminuted material which was also collected.

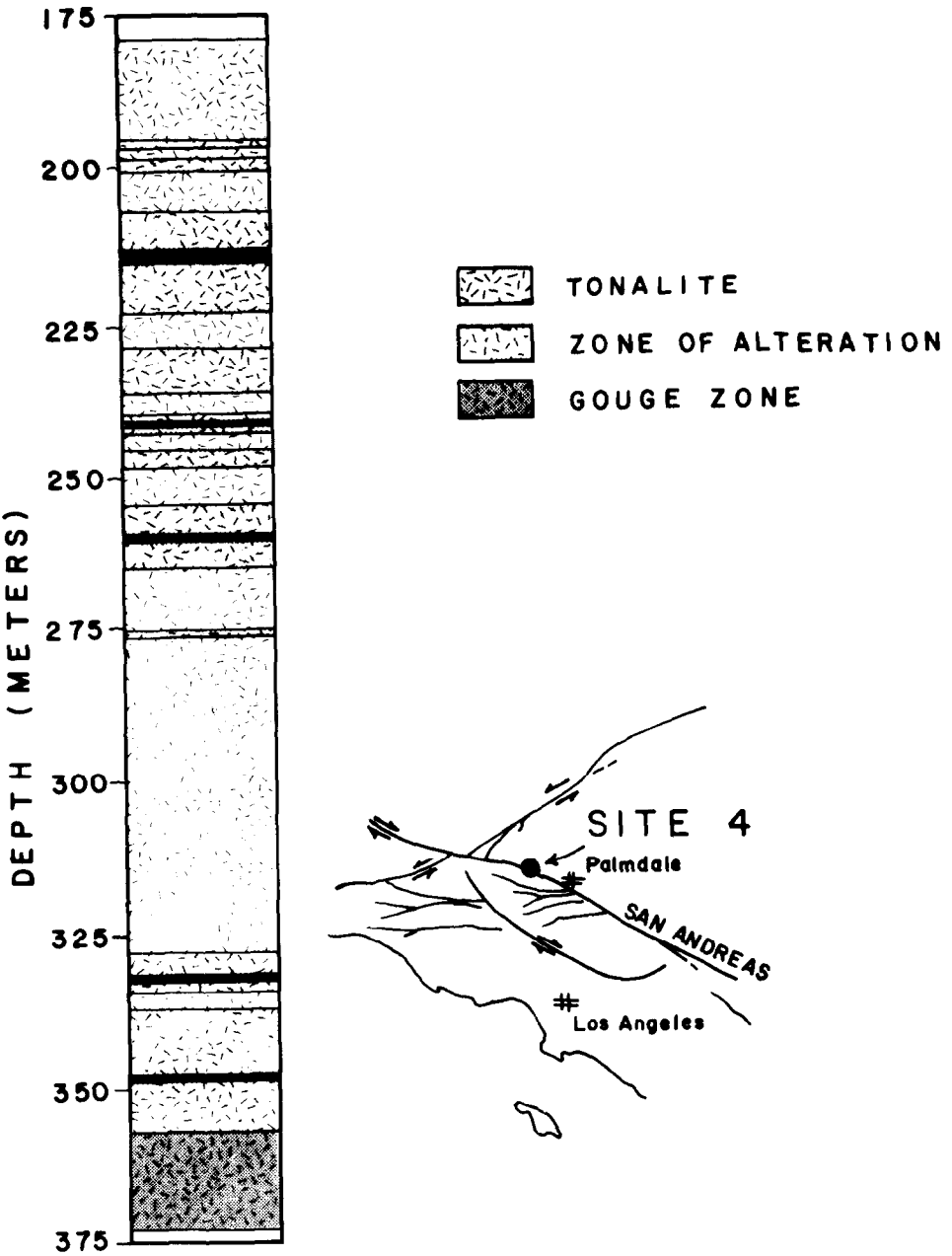

Fig. 2. Distribution of fault gouge within core retrieved from a Mesozoic tonalite pluton marginal to the San Andreas fault system. Note zones of alteration enclosing the six gouge zones. Attitude of gouge zones are high angle (shown horizontal for clarity).

Site 3 occurs as fresh roadcuts at Tejon Pass where gouge is developed from a range of parent rocks including granite pegmatite, diorite, and sedimentary rocks. Gouge formation at this site is less well developed, but it is

TABLE I

List of samples analyzed

Sample no.	Parent rock	Occurrence
(A) Gouge Samples from Painted Canyon		
PC-1	granite-gneiss	gouge zone in Painted Canyon fault
PC-2	granite-gneiss	gouge zone in Painted Canyon fault
PC-3	granite-gneiss	gouge zone in Painted Canyon fault
PC-4	granite-gneiss	gouge zone in Painted Canyon fault
(B) Gouge Samples from Big Pines, Site 2		
BP-1	granite gneiss	massive gouge zone
BP-2	applitic dike	same, dike in gneiss
BP-3	black comminuted rock	cm thick shear zone in gneiss
BP-4	pelona schist (?)	fault slice
BP-5	granite gneiss	fault slice
(C) Gouge samples from Tejon Pass, Site 3		
TP-1	tonalite	fault slice
TP-2	diorite	same unit as TP-1
TP-3	granite pegmatite	dike rock in TP-2
TP-4	clastic sed. rock	fault slice
TP-5	clastic sed. rock	fault slice
TP-6a	tonalite	fault slice, incipient gouge development
TP-6b	tonalite	same unit as TP-6a, moderate gouge dev.
TP-6c	tonalite	same unit as TP-6a, most intense gouge development
TP-7	diorite	same unit as TP-1
TP-8	quartz diorite	fault slice

(D) Tonalite and derived gouge from Core LH-2, Site 4

	Depth		Physical state
	(m)	(ft)	
2-11	205.7	675	mildly altered
2-12	213.1	699	gouge
2.13A	214.3	703	altered,friable
2-13B	214.6	704	gouge
2-27	260.0	853	gouge
2-33	278.9	915	pristine (fresh)
2-41	317.0	1040	mildly altered
2-46	331.0	1086	altered, friable, minor gouge
2-51A	349.0	1145	mildly altered
2-52B	353.3	1159	altered, friable
2-52C	361.8	1187	gouge
2-53B	367.6	1206	gouge
2-54A	372.5	1222	gouge

possible to see a range of gouge development in the field. Samples TP-6a, TP-TP-6b, and TP-6c demonstrate the transition from incipient to more complete gouge formation. It is interesting that despite the extensive development of gouge, relict textures are evident in all samples. For example, sample TP-3 was derived from a pegmatite dike traversing a diorite. Although this rock, as well as the enclosing diorite, powders to silt-size particles upon touch, the relict "ghost" of its original texture indicate a primary pegmatite grain size of several centimeters. Likewise, the relict diorite texture depicts a medium-grained, equigranular intergrowth of plagioclase and mafic silicate with an original grain size of 2—4 mm. The different units comprising the site occur in fault slices.

Site 4 is located just north of the San Andreas fault in the Lake Hughes area. We used a core retrieved from a 370 m drill hole into a tonalite pluton. This site allowed us to evaluate incipient gouge development in a relatively homogeneous body of igneous rock. We were able to study changes that occur in samples that range gradationally from rather pristine igneous rock to its gouge equivalent. Moreover, it provided a basis to study gouge development as a function of depth (and increasing confining pressure). As shown in Fig. 2, six zones of gouge occur, each symmetrically enclosed within an alteration zone. There is very little shearing within the section as main displacement appeared to be confined to the interface of gouge and its wallrock. As described below, the original tonalite consists of plagioclase (calcic oligoclase to sodic andesine), quartz, alkali feldspar, biotite, hornblende, and accessory minerals. Partial sericitization of feldspar and chloritization and oxidation of mafic silicates and oxides occur within the alteration zone. The samples analyzed range from "pristine" to "altered and friable" to "gouge" (Table I), relecting the relative degrees of alteration.

ANALYTICAL PROCEDURE

Each sample was partitioned with a sample splitter to obtain representative subsamples for the separate mineralogic, petrochemical and textural analyses.

The mineralogy of the fault gouge and related rocks was analyzed by optical examination of thin sections, X-ray diffraction, and electron microprobe. Half of each thin section was stained for K-feldspar and modal analyses involved duplicate measurements by two observers, each counting a minimum of 1500 points per thin section. X-ray examination of bulk samples and sample separates was done with a Philips-Norelco diffractometer with a focusing monochromator and using Cu K-alpha radiation. Scans were made a $1^\circ 2\theta$ per minute for all samples and at $\frac{1}{4}^\circ 2\theta$ per minutes over low angles of 2θ on all samples exhibiting alteration or cataclasis. Ultraslow scans were made to detect the nature of any existing clay minerals. X-ray analysis of grains utilized the Debye-Scherer powder camera. X-ray examination was made on bulk samples and upon sample separates. Samples were separated

first on the basis of the grain size by using 0.177, 0.149, and 0.063 mm sieves. Most of the samples also were sieved with a 0.044 mm screen in the hope of obtaining fine clays. In most samples, a very fine fraction was obtained by putting the whole sample into suspension and filtering out the fine suspensate.

Electron microprobe analysis was done on an automated, 3-channel MAC (Material Analysis Corporation) microprobe housed at the California Institute of Technology. Data collection and reduction were performed on-line by a Digital Corporation PDP-8/L computer utilizing the alpha correction factors of Albee and Ray (1970) and the empirical reduction scheme of Bence and Albee (1968). Operating conditions consisted of 15 kV accelerating potential, 0.05 μA current measured on brass and a 2—10 μm beam diameter. Oxides, synthetic silicates, and well characterized natural minerals were used as standards.

Textural analysis was preceded by placing each subsample in distilled water and exposing to high-intensity ultrasonic waves for 24 hours to facilitate particle disaggregation. Each subsample was then wet sieved through a 0.625 mm sieve to separate silt- and clay-size particles from coarser-grained ones. This step is required because silt- and clay-size materials were processed by the pipette method, whereas the coarser-grained materials were sieved. The details of these techniques are described in Carver (1971). Examination of grain thin-sections in the silt-size fraction indicated that the gouge had been successfully disaggreagated into constituent particles.

Petrochemical analysis of the samples was done for eight major (Si, Ti, Al, Fe, Mg, Ca, Na, and K), five minor or trace elements (Mn, Li, Rb, Sr, and Ba), and combined volatiles (H_2O and CO_2). Silicon was analyzed by UV—VIS colorimetric spectrophotometry. All other elements were analyzed by atomic absorption spectrometry using an HF-H_3BO_3 acid dissolution technique. Standards and blanks were made synthetically and U.S.G.S. reference samples were used as internal standards as a monitor of accuracy. Total volatile content was based on loss on ignition (L.O.I.) at 1000°C. For these samples, H_2O is the predominant volatile component with CO_2 as a very minor constituent.

Modal and grain-size distribution data are available from the authors upon request.

ANALYTICAL RESULTS

Petrography and petrofabric analysis

Thin section examination of numerous specimens of gouge derived from crystalline rocks from each of the four sites exhibit a surprisingly uniform fabric of angular (fragmented) grains of quartz, feldspar, hornblende, biotite, epidote, sphene, and magnetite distributed randomly in a very fine-grained, commonly structureless matrix (Fig. 3). There is no penetrative fluxion

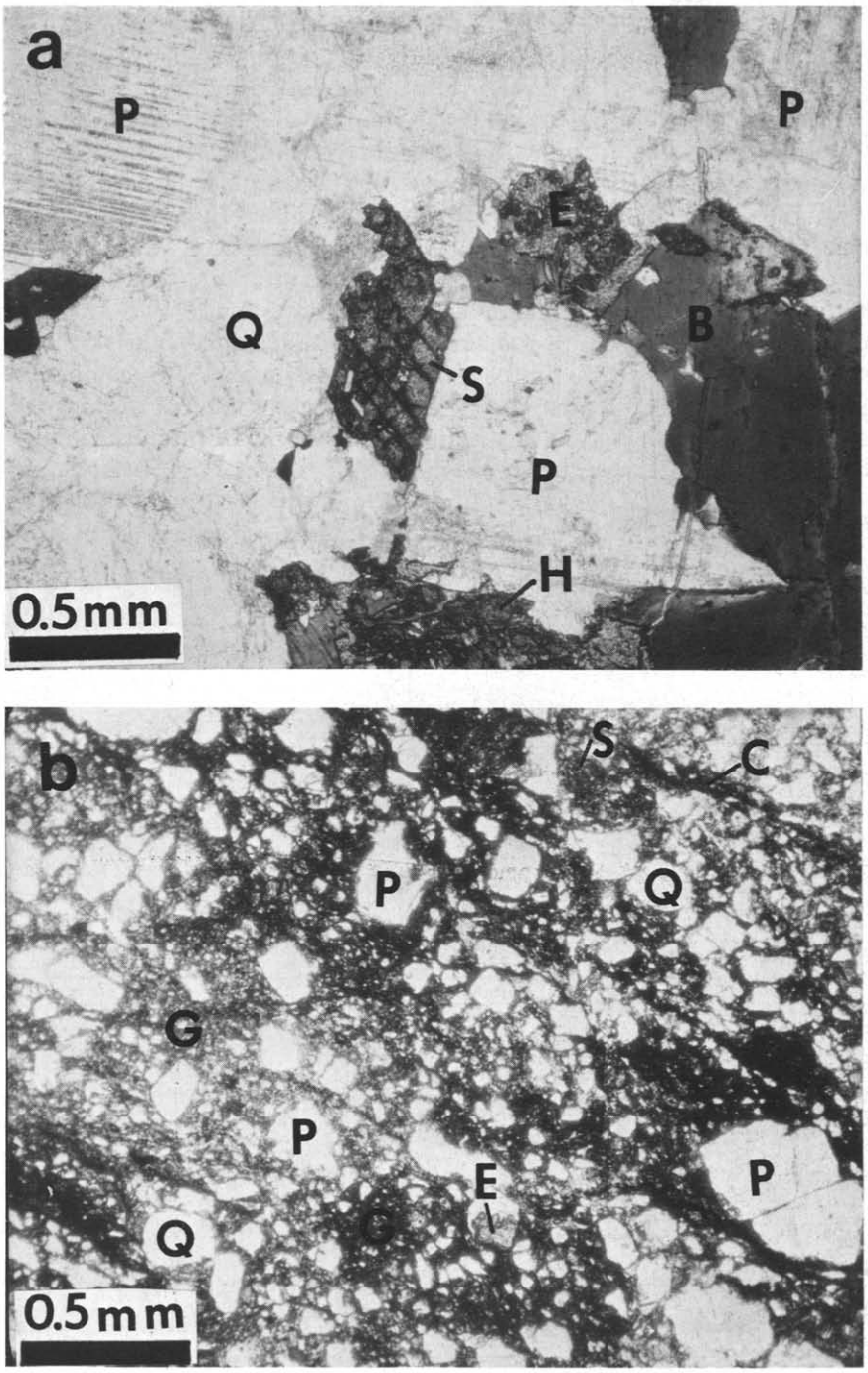

Fig. 3. a. Photomicrograph of Mesozoic tonalite, Site 4. Minerals include quartz (Q), plagioclase (P), biotite (B), hornblende (H), sphene (S), and retrograde epidote (E). b. Photomicrograph of gouge derived from tonalite. Numerous subangular fragments of quartz (Q), plagioclase (P), and sphene (S) are embedded in a gouge matrix (G, all fine-grained and dark areas) which is predominantly milled-down quartz and feldspar with minor chlorite (C), hematite and kaolinite.

structure and no evidence of any recrystallization with the exception of calcite and possibly chlorite. Fine-grained components of the gouge are almost universally derived directly from nearby large grains (porphyroclasts). Within the gouge, long monomineralic lenses of plagioclase, quartz, or K-feldspar suggest that often crystals have been disrupted completely and ground to gouge with little mixing of one mineral with the fragments of others. Where the gouge does involve a mixture of one mineral with another, such areas can commonly be related to the immediate juxtaposition of the two minerals occurring as large clasts on opposite sides of the finer gouge. Variations in modal composition can be directly related to the parent rock. Gouge derived from pegmatite and aplite consist almost exclusively of subequal portions of quartz and two feldspars (Fig. 4A) with minimal amounts of mafic silicate or Fe—Ti oxides. Gouge derived from tonalite to diorite is comprised dominantly of plagioclase, and lesser amounts of quartz, biotite hornblende, sphene, and Fe—Ti oxides (Fig. 4B). Zones of intense cataclasis often have

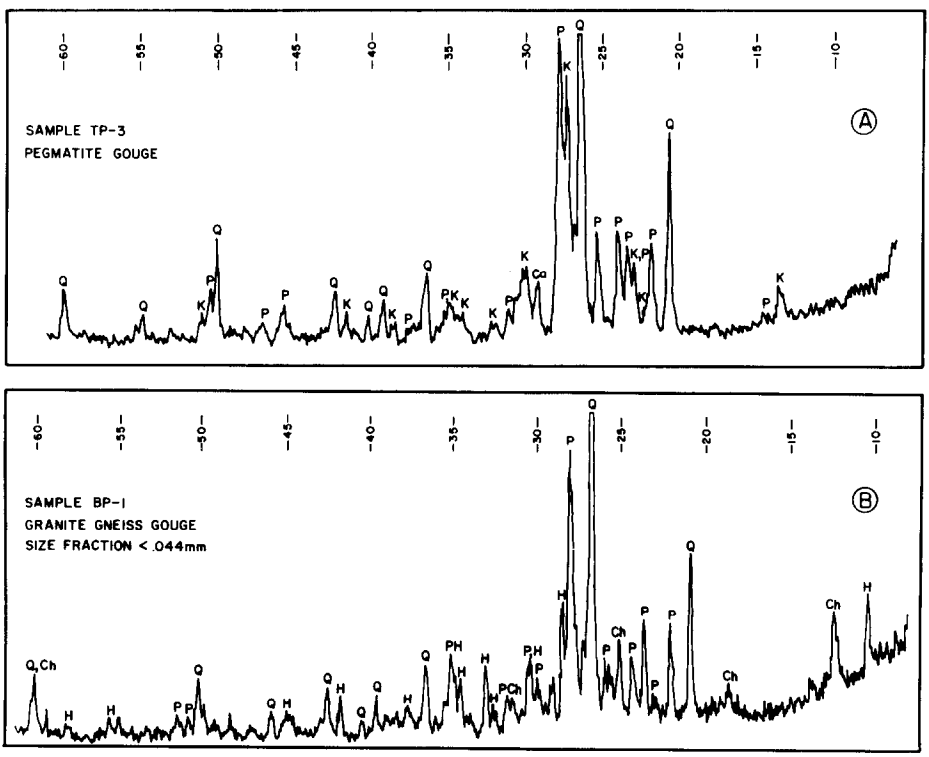

Fig. 4. X-ray diffractograms for sample TP-3 (Gouge derived from granite pegmatite) and for a size fraction less than 0.044 mm for sample BP-1 (Gouge derived from granitic gneiss). Mineral symbols are the same as in Fig. 3 except for K-feldspar (*K*) and chlorite (*Ch*).

more severe alteration resulting in sericitization of feldspars and replacement of hornblende and biotite by chlorite, hematite, and calcite. Epidote is a common mineral in the gouge but appears to have formed prior to cataclasis by retrogression of the original igneous or metamorphic mineralogy.

Sedimentary rock occurs in one area at the Tejon Pass site. This rock is cataclastically deformed and shows the only clear evidence of mixing of different lithologies in gouge development. Lithic fragments are mainly finely laminated siltstone with lesser amounts of large quartz or feldspar grains and less abundant knots of medium grained plagioclase. The matrix consists of cataclastically deformed siltstone. Knots of siltstone and crushed rock cemented with carbonate occur within the matrix. The mineralogy of the siltstone-derived clay gouge is more complex than that of the "crushed rock" gouges previously discussed. Fine-grained clay material rich in iron oxides, abundant calcite veining, and zeolite rosettes occur in distinctive segregations. Like the gouges derived from igneous rocks, most of the gouge is medium to fine-grained and shows little evidence of large scale translational movement. The gouge appears to have gone through several stages of development, for occasionally one can find coherent clasts with a mineralogy and texture of fine gouge.

Structures which suggest major movement are rare but occur in several thin sections examined. These features are through-going, very fine-grained zones which are not crossed by fragments of larger clasts. They thus cut through the main cataclastic portions of the rock. Usually, the grain size is too fine for optical identification, but in some places the larger grains within these zones show the presence of plagioclase, quartz, and chlorite.

The study of grain surface microtextures of 76 grains of quartz in the gouge matrix of 5 samples by scanning electron microscopy show that quartz grains remain angular even in the most cataclasized material. This supports the contention of Logan (1977) that ploughing of asperties (surface irregularities) is not a major mechanism in the generation of gouge. The grains observed are generally subangular to angular, somewhat elongate with rough, hackly surfaces, although a few samples (specifically those from Big Pines) contained grains which are subrounded to rounded, and subspherical with smooth undulatory topography. The grains examined include a wide variety of surface microtextures including fracture and breakage surfaces, surfaces related to chemical deposition of silica, and crystallographically oriented chemical and diagenetic etching, smooth undulatory topography, and unoriented fractures. It is difficult to generalize regarding the relative frequency of other microtextures due to the small sample size, but chemical etching with crystallographic orientation and unoriented fractures are present in most samples. An exception is BP-4 (gouge derived from the Pelona Schist) where smooth undulatory topography dominates. Chemical deposition of silica is second most frequent in the Lake Hughes and Big Pines samples, but chemical etching with crystallographic orientation is second in the samples from the Painted Canyon area.

X-ray mineralogy

Due to the limiations of X-ray diffraction, it is not possible to clearly detect a mineral which is less than about 3% in abundance in the sample. Thus sample separations aimed at concentrating certain phases relative to others are of major importance. Separations on the basis of size fraction were expected to show major differences in mineralogy based on the assumption that clays and other alteration products would be more common in the finer size fractions. Samples were analyzed as a whole and for the finer fractions less than 0.044 mm. There was consistently no change in the X-ray diffractograms as a function of grain size as shown in Fig. 4B, which is the finest size fraction separated from granite gneiss gouge. In all cases, the major minerals detected by X-ray are quartz, plagioclase, chlorite, hornblende, biotite, potassium feldspar and Fe—Ti oxides. The ratios of these, as measured by peak height, did not change as a function of grain size, and change noticeably only for fractions which were separated on the basis of magnetic properties.

Superimposed upon the peaks related to the major minerals are lesser peaks caused by the presence of calcite, epidote, and rarely actinolite. Clay, commonly absent, occurred in small amounts in a few samples and is kaolinitic and generally not very well crystallized.

Mineral chemistry

Electron microprobe analysis of mineral constituents of protolith (sample 2-33) and derived gouge (sample 2-46) from the Lake Hughes core were completed to ascertain the effect of cataclasis on mineral composition. Thin section and X-ray examination (above sections) have shown that gouge formation at the four sites involves only minimal change in mineralogy. As a further evaluation, microprobe analysis was done to see if the relict minerals in the gouge, by comparison to the protolith, experienced any chemical change during gouge formation. The Lake Hughes core was chosen as both gouge and protolith occur. Sample 2-33 was chosen for the protolith due to its pristine nature, and gouge sample 2-46 was chosen on the basis of whole-rock chemistry as being the most similar to the idealized protolith. As is shown in the petrochemistry section (below), there is a natural (primary) compositional variation of the tonalite pluton from which this core was retrieved, and this specific gouge sample was chosen to preclude the effect of original compositional variation.

Table II reports the analysis of biotite, sphene, magnetite, alkali feldspar, and plagioclase from the protolith and derived gouge. In summary, the mineral compositions are indistinguishable. Moreover, in the case of feldspars (Fig. 5), there is no measurable difference in composition between larger mineral fragments and the very fine-grained fragments forming the gouge matrix. The biotites are intermediate between annite and phlogopite with

TABLE II

A. Electron microprobe analyses of alkali feldspar from protolith and derived gouge from the San Andreas fault at Lake Hughes

Sample:	2.33.7	2.46.4	2.46.1	2.46.7	2.46.8	2.46.5
SiO_2	64.86	63.24	64.28	65.20	65.24	65.34
Al_2O_3	18.32	18.37	18.45	18.93	18.22	18.88
TiO_2	0.00	0.03	0.00	0.01	0.00	0.04
FeO	0.06	0.04	0.03	0.03	0.11	0.03
MgO	0.00	0.00	0.00	0.00	0.00	0.00
BaO	0.56	0.72	1.17	0.79	0.60	0.73
CaO	0.00	0.46	0.00	0.00	0.00	0.01
Na_2O	0.86	1.41	0.71	1.15	0.92	1.01
K_2O	15.52	13.89	15.41	15.13	15.56	15.47
Total	100.18	98.14	100.05	101.25	100.66	101.51
Si	2.997	2.976	2.986	2.981	3.002	2.983
Al	0.998	1.019	1.011	1.020	0.989	1.016
Ti	0.000	0.001	0.000	0.000	0.000	0.001
Fe	0.002	0.001	0.001	0.001	0.004	0.001
Mg	0.000	0.000	0.000	0.000	0.000	0.000
Ba	0.010	0.013	0.021	0.014	0.011	0.013
Ca	0.000	0.023	0.000	0.000	0.000	0.0002
Na	0.077	0.129	0.064	0.102	0.082	0.089
K	0.915	0.834	0.913	0.883	0.914	0.901
Or	92.27	83.45	91.46	88.35	90.72	89.78
Ab	7.71	12.89	6.40	10.24	8.19	8.89
An	0.00	2.32	0.00	0.00	0.00	0.02
Cn	1.02	1.33	2.14	1.41	1.09	1.31
Remarks [c]	P-C	G Pc	G-Pc	G-Pc	G-M	G-M

B. Electron microprobe analysis of plagioclase from protolith and derived gouge from the San Andreas fault at Lake Hughes

Sample:	2-33P2A	2-33-8	2-33P4A	2-33P3A	2-33-2	2-33-4	2-33-9	2-33-1
SiO_2	61.18	60.98	61.19	60.44	60.64	59.70	60.46	59.41
Al_2O_3	25.08	24.82	25.21	24.81	25.39	25.13	25.29	25.51
TiO_2	0.00	0.00	0.01	0.00	0.00	0.03	0.00	0.05
FeO	0.07	0.13	0.07	0.13	0.17	0.19	0.13	0.09
MgO	0.05	0.00	0.02	0.07	0.00	0.00	0.00	0.00
BaO	0.00	0.00	0.00	0.00	0.00	0.00	0.03	0.03
CaO	5.74	6.12	6.06	5.85	6.78	6.78	7.03	7.07
Na_2O	7.61	7.93	7.98	7.61	7.55	7.69	7.65	7.53
K_2O	0.13	0.37	0.14	0.05	0.58	0.27	0.22	0.34
Total	99.95	100.35	100.70	99.04	101.10	99.78	100.82	100.03
Si [b]	2.712	2.704	2.698	2.706	2.676	2.670	2.674	2.654
Al	1.310	1.298	1.310	1.309	1.321	1.325	1.319	1.343
Ti	0.000	0.000	0.000	0.000	0.000	0.001	0.000	0.002
Fe	0.002	0.005	0.002	0.005	0.006	0.007	0.005	0.003
Mg	0.004	0.000	0.001	0.004	0.000	0.000	0.000	0.000
Ba	0.000	0.000	0.000	0.000	0.000	0.000	0.001	0.001

TABLE IIB (continued)

Sample:	2-33P2A	2-33-8	2-33P4A	2-33P3A	2-33-2	2-33-4	2-33-9	2-33-1
Ca	0.273	0.290	0.286	0.281	0.321	0.325	0.333	0.338
Na	0.654	0.682	0.683	0.660	0.646	0.666	0.657	0.652
K	0.007	0.021	0.008	0.003	0.032	0.015	0.012	0.020
An	29.20	29.24	29.30	29.72	32.10	32.28	33.24	33.50
Ab	70.01	68.66	69.87	69.97	64.65	66.22	65.51	64.56
Or	0.79	2.10	0.83	0.31	3.25	1.50	1.25	1.94
Remarks [c]	P-Rim	P-Rim	P-Rim	P-Rim	P	P	P	P

[a] All Fe as FeO.
[b] Formula units per five cations.
[c] P = protolith, G = gouge, Pc = porphyroclast, M = matrix.

Samples:	2-33-3	2-33-7	2-33-5	2-33P3B	2-46P1A	2-46P1AZ	2-46-1
SiO_2	59.48	59.48	59.17	56.81	60.44	60.05	59.95
Al_2O_3	25.53	25.51	25.64	27.45	24.72	24.99	24.62
TiO_2	0.04	0.01	0.03	0.00	0.04	0.18	0.00
FeO	0.18	0.12	0.13	0.13	0.07	0.02	0.05
MgO	0.00	0.00	0.00	0.00	0.04	0.00	0.00
BaO	0.02	0.00	0.04	0.00	0.00	0.00	0.00
CaO	7.45	7.59	7.75	8.85	5.92	6.26	6.39
Na_2O	7.40	7.27	7.13	6.16	7.83	8.16	7.83
K_2O	0.42	0.24	0.32	0.13	0.13	0.07	0.19
Total	100.50	100.21	100.20	99.61	99.31	99.81	99.03
Si	2.648	2.651	2.641	2.555	2.703	2.680	2.694
Al	1.340	1.340	1.349	1.355	1.303	1.314	1.305
Ti	0.001	0.000	0.001	0.000	0.001	0.006	0.000
Fe	0.007	0.004	0.005	0.005	0.003	0.001	0.002
Mg	0.000	0.000	0.000	0.000	0.003	0.000	0.000
Ba	0.000	0.000	0.001	0.000	0.000	0.000	0.000
Ca	0.355	0.362	0.371	0.427	0.284	0.300	0.308
Na	0.639	0.628	0.618	0.537	0.679	0.706	0.682
K	0.024	0.013	0.018	0.008	0.008	0.004	0.011
An	34.91	36.1	36.84	43.93	29.23	29.65	30.74
Ab	62.75	62.57	61.38	55.29	70.00	69.94	68.18
Or	2.34	1.33	1.78	0.78	0.77	0.41	1.09
Remarks	P	P-Core	P-Core	P-1 Core	G-Pc	G-Pc	GPc

Sample:	2-46-4	2-46-9	2-46-3	2-46-5	2-46-7	2-46-5	2-46-8
SiO_2	59.52	60.81	60.26	60.24	59.79	61.84	61.18
Al_2O_3	24.69	25.24	24.82	25.19	25.76	24.24	25.29
TiO_2	0.11	0.00	0.00	0.01	0.06	0.01	0.00
FeO	0.20	0.12	0.18	0.10	0.14	0.02	0.08
MgO	0.03	0.00	0.00	0.00	0.01	0.00	0.00

TABLE IIB (continued)

Sample:	2-46-4	2-46-9	2-46-3	2-46-5	2-46-7	2-46-5	2-46-8
BaO	0.00	0.00	0.02	0.05	0.00	0.01	0.00
CaO	6.39	6.59	7.08	7.22	7.33	5.61	6.85
Na_2O	7.66	7.82	7.59	7.53	7.52	7.27	8.01
K_2O	0.29	0.24	0.25	0.25	0.20	0.46	0.14
Total	98.89	100.82	100.19	100.58	100.82	99.45	101.55
Si	2.684	2.685	2.683	2.672	2.649	2.750	2.684
Al	1.313	1.314	1.303	1.318	1.346	1.271	1.308
Ti	0.004	0.000	0.000	0.000	0.002	0.000	0.000
Fe	0.008	0.005	0.007	0.004	0.005	0.001	0.003
Mg	0.000	0.000	0.000	0.001	0.000	0.000	0.000
Ca	0.309	0.312	0.338	0.343	0.348	0.267	0.320
Na	0.670	0.670	0.655	0.648	0.647	0.627	0.682
K	0.017	0.014	0.014	0.014	0.011	0.026	0.008
An	31.01	31.33	33.55	34.13	34.60	29.06	31.83
Ab	67.30	67.29	65.06	64.45	64.29	68.14	67.41
Or	1.69	1.38	1.39	1.42	1.10	2.80	0.76
Remarks	GPc	GPc	GPc	GPc	GPc	G-M	G-M

TABLE IIC

Electron microprobe analyses of biotite, sphene, and magnetite, and protolith and derived gouge from the San Andreas fault at Lake Hughes

	Biotite		Sphene		Magnetite			
Sample:	2-33-04	2-46-03	2-33-1	2-46-6	2-33P1A	2-33-1	2-46P1D	2-46-03
SiO_2	36.18	36.10	30.94	30.75	0.13	0.07	0.06	0.03
Al_2O_3	15.62	15.58	0.95	1.42	0.00	0.00	0.07	0.00
Cr_2O_3	—	—	—	—	—	0.01	—	0.03
Ce_2O_3	—	—	0.25	0.37	—	—	—	—
TiO_2	2.20	1.67	37.72	36.60	0.09	0.06	0.00	0.04
FeO	19.96	20.29	1.00	1.80	93.62	94.61	94.27	95.93
MgO	11.89	11.18	0.00	0.05	0.00	0.02	0.01	0.00
MnO	0.42	0.33	0.16	0.12	0.17	0.09	0.07	0.06
ZnO	0.05	0.10	—	—	—	0.03	—	0.00
CaO	0.10	0.00	28.28	28.12	0.09	—	0.00	—
Na_2O	0.05	0.16	—	—	0.03	—	0.01	—
K_2O	9.02	9.78	—	—	0.00	—	0.00	—
F	0.51	0.66	0.40	0.61	—	—	—	—
Cl	0.02	0.04	—	—	—	—	—	—
Total	95.79	95.59	99.53	99.58	94.13	95.00	94.47	96.09
Si [a]	2.782	2.817	1.011	1.004	0.007	0.002	0.002	0.001
Al^{IV}	1.218	1.183	0.000	0.000	0.000	0.000	0.000	0.000
Al^{VI}	0.197	0.250	0.036	0.055	0.000	0.000	0.003	0.000
Cr	—	—	—	—	—	0.000	—	0.001
Ce	—	—	0.003	0.004	—	—	—	—

TABLE IIC (continued)

	Biotite		Sphene		Magnetite			
Sample:	2-33-04	2-46-03	2-33-1	2-46-6	2-33P1A	2-33-1	2-46P1D	2-46-03
Ti	0.127	0.098	0.927	0.899	0.002	0.002	0.000	0.001
Fe	1.284	1.324	0.027	0.049	2.972	2.989	2.987	2.995
Mg	1.362	1.300	0.000	0.002	0.000	0.001	0.000	0.000
Mn	0.027	0.021	0.004	0.003	0.005	0.003	0.002	0.002
Zn	0.003	0.006	—	—	—	0.001	—	0.000
Ca	0.009	0.000	0.990	0.984	0.004	—	0.000	—
Na	0.008	0.024	—	—	0.002	—	0.000	—
K	0.885	0.973	—	—	—	—	0.000	—
F	0.124	0.164	0.042	0.064	—	—	—	—
Cl	0.002	0.005	—	—	—	—	—	—
% E.M. [b]	42.79	44.13	97.60	96.23	99.33	99.63	99.75	99.83
Remarks	P	G	P	G-Pc	P	P	G	G

[a] Formula atoms on basis of 7 octahedral + tetrahedral cations (biotite); three cations (sphene and magnetite).
[b] % end member annite (Fe-end member, biotite), $CaTiSiO_3$ (sphene), Fe_3O_4 (magnetite), respectively.

mole fraction annite equal to 0.428 and 0.441 in the protolith and gouge, respectively. Concentrations of Al, Ti, Mn, F and other elements are also quite similar. Magnetite in both lithologies are essentially pure end-member Fe_3O_4. Likewise, sphene is largely stoichiometric with similar concentrations of the minor elements (Al, Mn, Fe, Ce, F). Primary alkali feldspar in the tonalite has the composition $Or_{91.3}$ $Ab_{7.7}$ $Cn_{1.0}$ (Cn = the celsian end member, $BaAl_2Si_2O_8$) with no detectable anorthite component. Large fragments of alkali feldspar in the derived gouge range from $Or_{88.4}$ $Ab_{10.2}$ $Cn_{1.4}$ to $Or_{91.5}$ $Ab_{6.4}$ $Cn_{2.1}$ and matrix feldspar has the compositional range $Or_{89.8}$ $Ab_{8.9}$. $Cn_{1.3}$, both with no detectable anorthite component. Plagioclase in the tonalite protolith is normally zoned and ranges in composition from $An_{29.2}$ $Ab_{68.7}$ $Or_{2.1}$ to $An_{36.8}$ $Ab_{61.4}$ $Or_{1.8}$; porphyroclasts of plagioclase in the gouge ranges from $An_{31.0}$ $Ab_{67.3}$ $Or_{1.7}$ to $An_{34.6}$ $Ab_{64.3}$ $Or_{1.1}$ while matrix plagioclase ranged from $An_{29.1}$ $Ab_{68.1}$ $Or_{2.8}$ to $An_{31.8}$ $Ab_{67.4}$ $Or_{0.76}$. The difference in composition of the porphyroclasts and matrix plagioclase, both of which fall in the range of composition found for the protolith, probably reflects the preferential fracturing of the originally more albitic rims of the primary zoned feldspar as opposed to the anorthitic cores.

Grain-size distribution

The results of the textural analyses for each of the four sites are presented as histograms in Figs. 6—9. The intrinsic features of the data are (1) most of

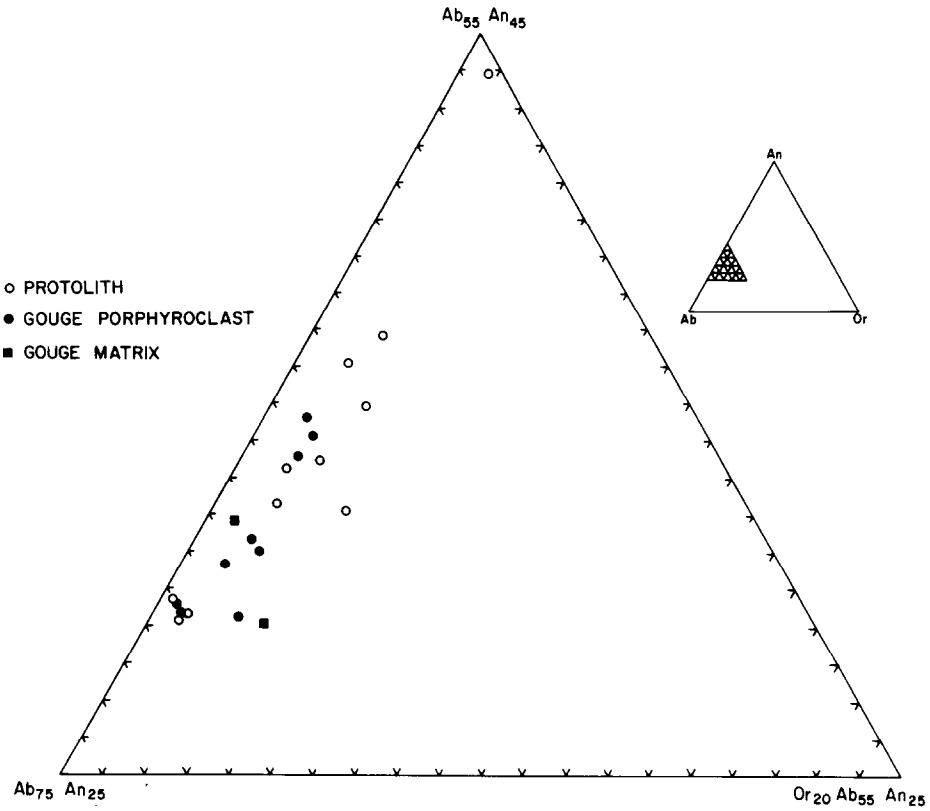

Fig. 5. Plagioclase compositions from tonalite and derived gouge, Site 4 (Core LH-2).

the particles fall in the sand and silt range, (2) there is a rather consistent size gap in the very fine sand-size category and (3) a shift in the principal mode from medium and fine sand to coarse, medium, and fine silt categories occurs with increasing cataclasis and with increasing depth.

With the exception of the data for the Tejon Pass locality (Fig. 8), the principal mode has a broad range from coarse sand to very fine silt size particles (0.008 to 2.0 mm). Clay-size particles are always less than 13 wt. % and average 5.3—7.25 wt. %. As shown above, this clay-size material is generally not of clay minerals but rather of very fine-grained particles of quartz, feldspar, hornblende and other minerals of the original igneous or metamorphic parent rock (Fig. 4B).

For some sites there are size gaps in the coarse and medium sand-size categories (sites 3 and 4) but of particular interest is the consistent gap from 0.06 to 0.09 mm (very fine-grained sand). There is considerable debate in sedimentology regarding the apparent paucity of particular grain sizes produced in nature (Pettijohn, 1975, pp. 41—45). The problem centers on whether the dearth of certain particle sizes are real or an artifact of analyti-

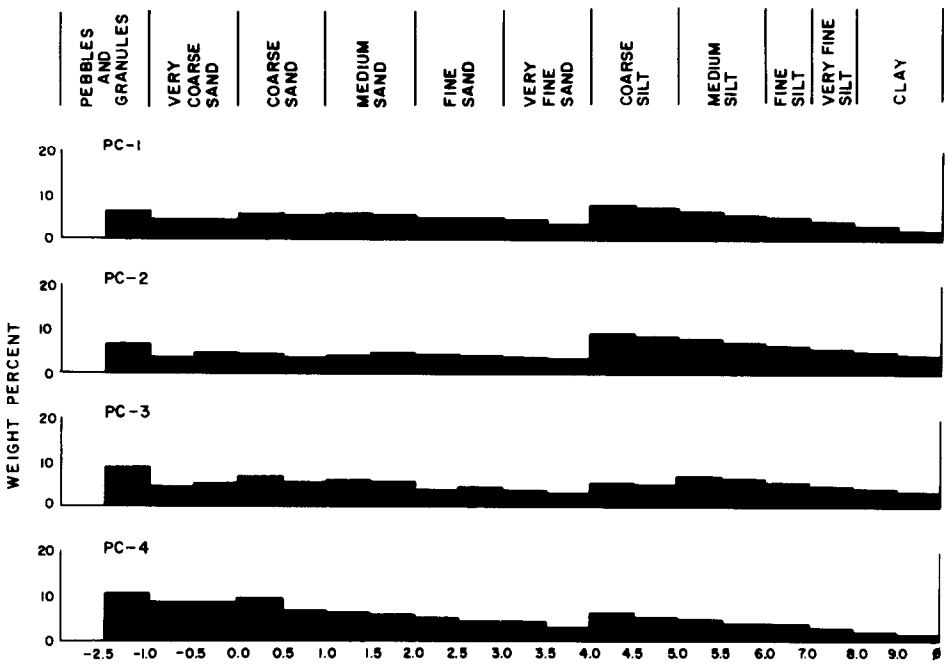

Fig. 6. Histograms showing grain-size distribution of samples from Painted Canyon area. The diameter of grains is represented by phi (ϕ) units which correlate to millimeters by mm $= \frac{1}{2}\phi$.

cal technique. Although this debate has not been extended to intrafault materials, it is necessary to test the reality of such apparent size gaps by another analytical procedure to determine whether or not the apparent paucity of material is due to instrumental technique. Attention was directed to study this size gap in the samples from site 4, core LH-2, because (1) this is the size fraction where analytical technique changes from sieving to pipette analysis and (2) it is likely that the tonalite protolith comprising much of this core is lithologically and texturally more homogeneous than protolith at other sample localities.

An average of 612 grain diameters were measured from photomicrographic negatives from each of two grain size fractions for seven samples by means of a Zeiss TGZ particle-size analyzer. The particle-size analyzer was used in the standard range mode in conjunction with the linear distribution mode to show at what sizes maxima occur. Measurement of grain diameters by this method shows that coarse-grained silt is dominant over very fine-grained sand in all seven samples. The modal difference between these two size fractions is about 30%. Textural data obtained by sieving and pipette analysis (weight percentages) are not directly comparable with particle-size measurements obtained from thin sections (apparent frequency percent), but both methods record an obvious textural gap in the very fine-grained sand

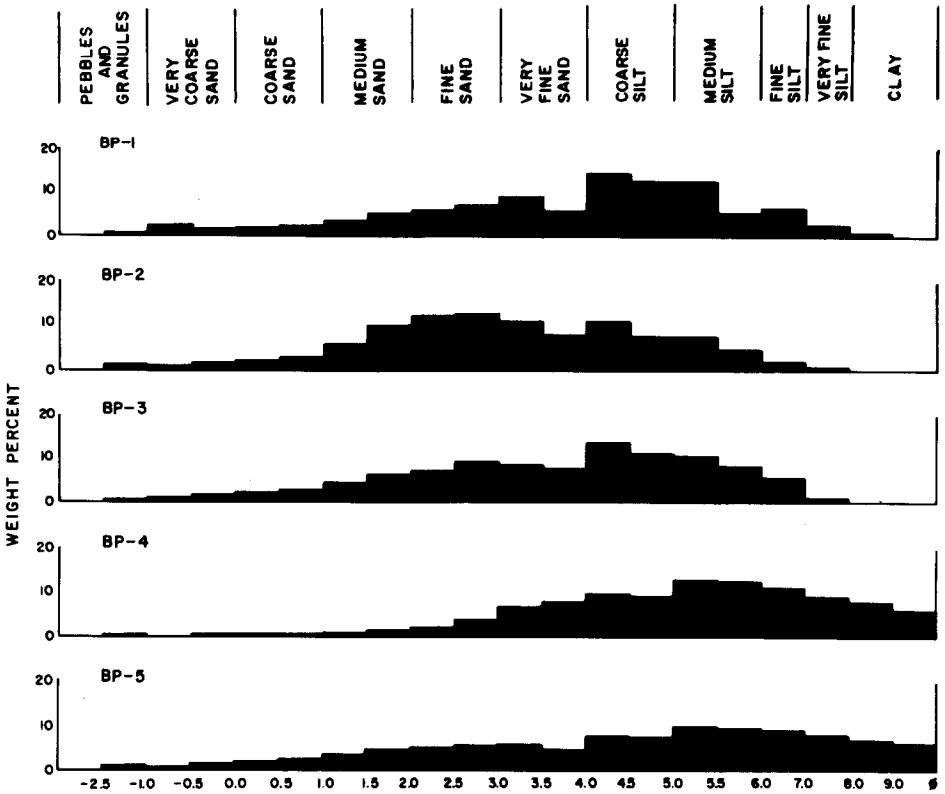

Fig. 7. Histograms showing grain-size distribution of samples from Big Pines area.

fraction. Consequently we regard this size gap as a real and pertinent feature of the fault gouge. Particle-size gaps in fault gouge also were observed by Engelder (1974) who attributed it to incomplete cataclasis. We quite agree with this conclusion. A secondary contributing factor may be the nature of quartz breakage. Quartz breakage occurs both by conchoidal fracture and by rhombohedral parting on $\{10\bar{1}1\}$ or $\{01\bar{1}1\}$. Scanning electron microscopy of sand-to silt-size quartz grains by Krinsley and Smalley (1973) and Margolis and Krinsley (1974) show that conchoidal fracture is the dominate mode of breakage for grains greater than 0.5 mm in diameter, but that parting becomes dominant for grain sizes less than 0.1 mm. In other words, as angular quartz grains attain a grain size equal to that of very fine sand (3—4 ϕ or 0.0625—0.125 mm) or less, the grain shapes change from being blocks to flat plates. Our observed gap falls at the lower limits of this transition from fracture to parting behavior. Grains within this transitional size group have higher structural instability as both breakage mechanisms are equally operative. Hence, fewer particles will exist in this size range and a grain-size gap, such as that we observe, will be generated.

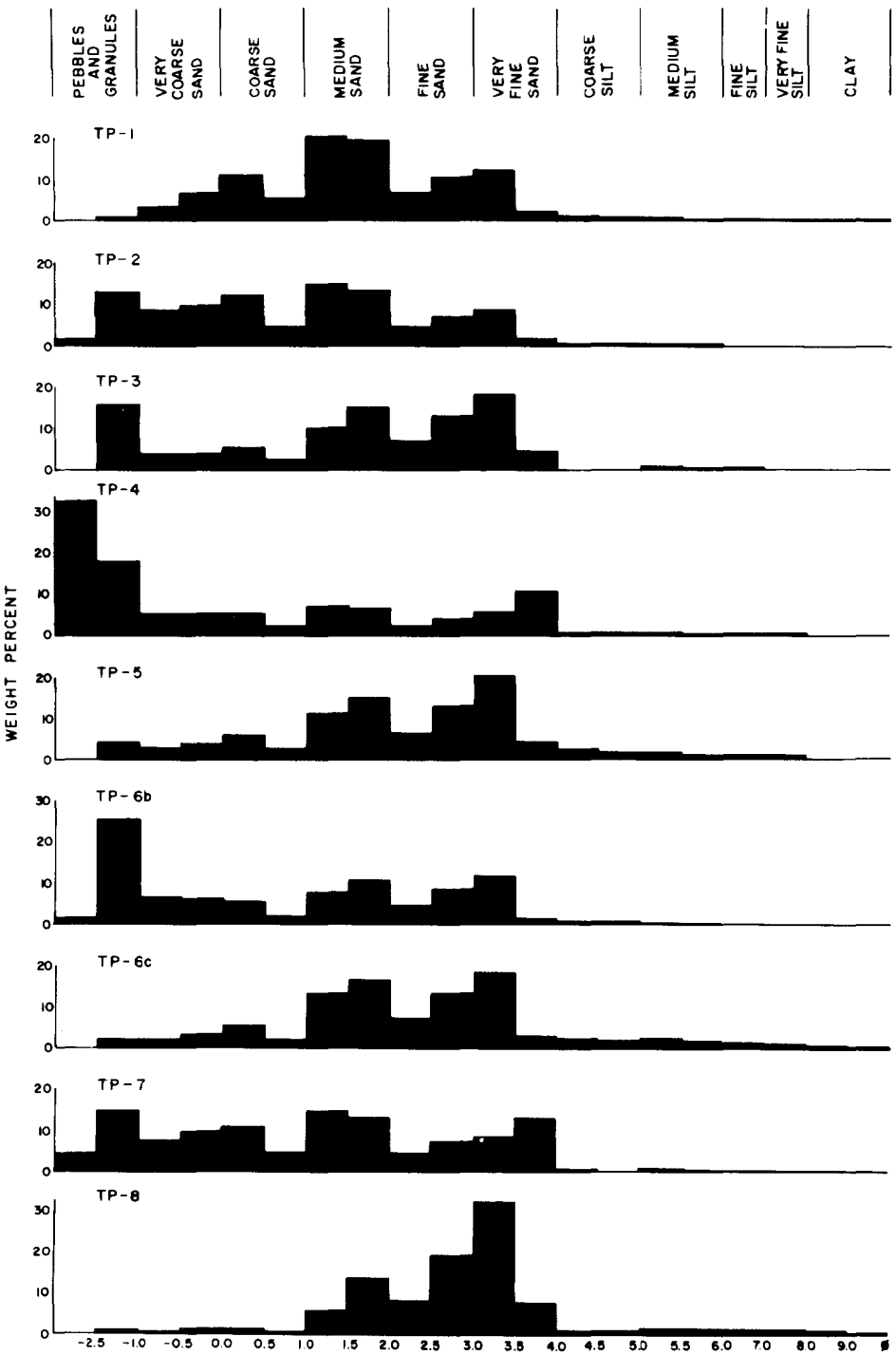

Fig. 8. Histograms showing grain-size distribution of samples from Tejon Pass area.

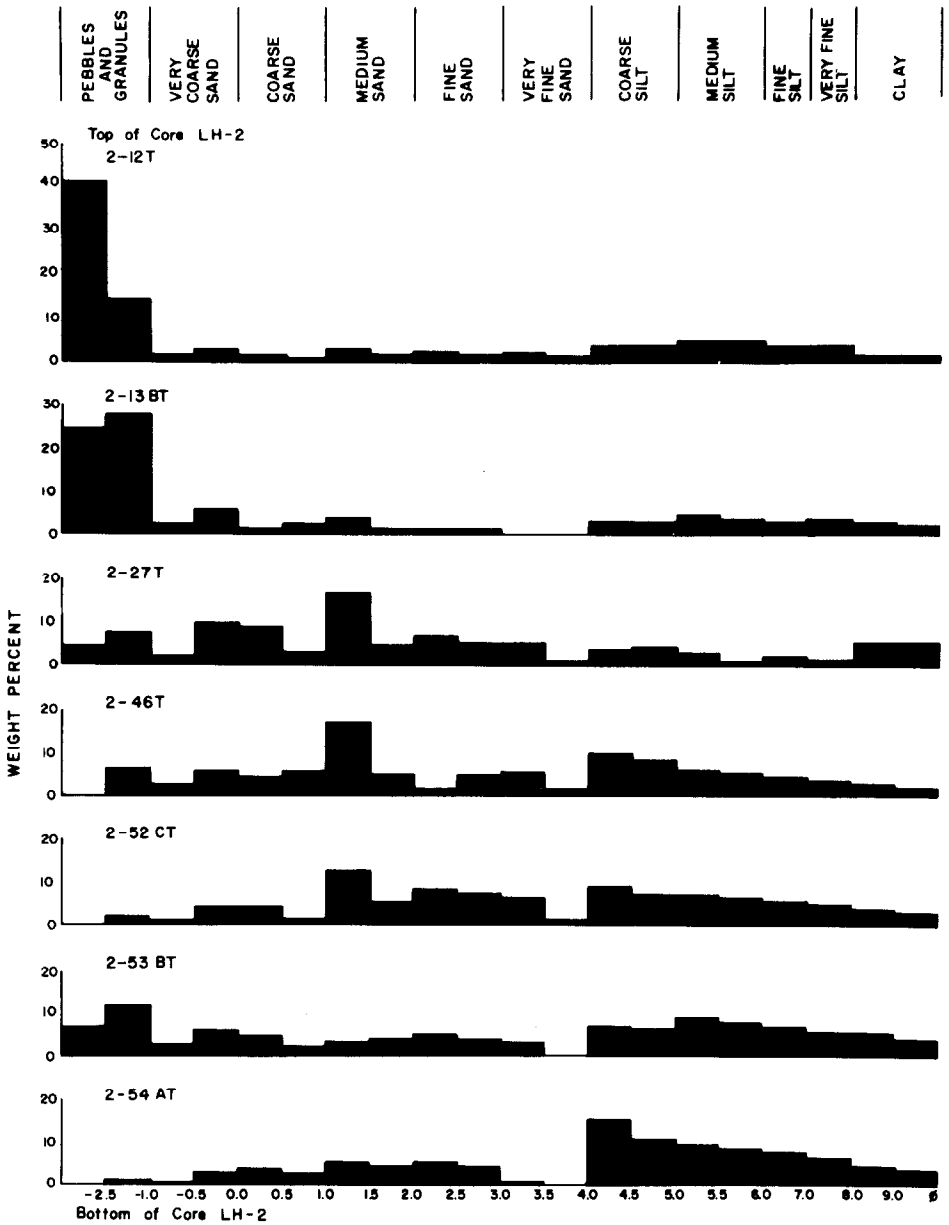

Fig. 9. Histograms showing grain-size distributions of samples from core LH-2, Lake Hughes area.

Data for Tejon Pass (Site 3) abruptly terminate at this gap (Fig. 8), thus suggesting that cataclasis at this site is far less complete than at the remaining three sites. Of interest are samples TP-6b and TP-6c which were collected as part of a sequence representing increasing comminution with gouge develop-

ment. From the histogram (Fig. 8), a shift of a principal mode in the granule and coarse sand range to medium, fine, and very fine sand is clearly evident as well as detectable contribution to the silt- and clay-size categories.

Gouge specimens form site 4 (core in tonalite at Lake Hughes) allow evaluation of size distribution as a function of depth. The weight percentages of clay-size (not clay mineralogy) material is variable from 3.74 to 11.11, but show no consistent pattern with increasing depth. Although somewhat variable, silt-size material generally increases with depth. Sand-size material systematically increases from samples 2-12T through 2-27T, and then systematically decreases throughout the remainder of the core. In a complimentary fashion, silt-size particles consistently increase in amount from 14.9 to 57.6 wt.% from the upper third to the bottom of the core. Granule- and pebble-size material generally decreases in weight percentage with depth. It seems that grain size and sorting of intrafualt material decrease as a function of increasing confining pressure (Engelder, 1974; Ayden, 1977). The samples from core LH-2 generally show a decrease in overall grain size with depth;

TABLE III

Comparison of mineral composition of medium-grained sand (0.25—0.50 mm) and coarse-grained silt (0.031—0.0625 mm) site fractions of fault gouge from Core LH-2, Lake Hughes

Mineral composition	Sample no.							
	2-12T	2-13BT	2.27T	2-46T	2-52CT	2-53BT	2-54AT	Mean
A. Medium sand fraction								
Quartz	38.6	29.4	22.2	25.0	24.4	23.2	22.2	26.4
Plagioclase	42.2	42.2	54.2	54.6	60.2	57.0	50.0	51.4
Microcline	2.2	1.2	1.0	0.4	0.2	0.8	2.4	1.2
Rock fragments	21.4	23.0	20.2	17.6	12.2	14.8	22.8	18.8
Calcite	1.6	1.6	1.4	0.6	1.0	0.2	1.6	1.2
Chlorite	0.8	0.6	0.2	0.8	0.0	0.8	0.2	0.5
Biotite	0.8	0.0	0.0	0.0	0.0	0.4	0.0	0.2
Hornblende	7.2	1.2	0.4	1.0	0.4	2.2	0.4	1.8
Fe-Ti Oxides	2.0	0.8	0.4	0.0	1.6	0.6	0.4	0.8
B. Coarse silt fraction								
Quartz	36.3	41.3	28.3	27.0	18.0	17.0	21.7	27.0
Plagioclase	38.0	45.3	52.0	52.3	51.3	55.0	61.7	51.0
Microcline	0.0	0.3	0.0	0.0	0.0	0.0	0.0	0.0
Rock fragments	8.7	2.3	1.3	2.0	2.0	1.3	1.7	2.8
Calcite	3.7	1.7	2.0	1.0	3.7	2.7	1.0	2.3
Chlorite	1.7	0.3	0.7	1.0	1.0	0.0	1.0	0.8
Biotite	0.0	0.0	0.0	0.3	0.0	0.3	0.0	0.1
Hornblende	9.0	4.3	8.0	12.3	8.0	8.0	7.7	8.0
Fe-Ti Oxides	2.7	4.0	7.7	4.0	16.0	15.7	5.3	8.0

[a] Values expressed as number percentages.

however, the sorting is poor throughout the sampled depth.

The modal composition of quartz and plagioclase in the seven Lake Hughes gouge samples appear to be independent of texture for the medium-grained sand and coarse-grained silt fractions (Table III). The modal percentage of rock fragments decreases with decreasing grain size as is expected, whereas the percentages of iron titanium oxides and hornblende increase with decreasing grain size. These differences probably reflect breakage of these grains during gouge generation. The consistency of quartz and plagioclase between these two size fractions is somewhat puzzling. One might expect an increase in the percentage of plagioclase with decreasing grain size due to the volumetric dominance of this mineral in the protolith and its relative mechanical instability.

Cumulative curves for each sample were plotted on both logarithmic normal and extreme value probability graph paper. These density functions were suggested by the general shapes of the histograms shown in Figs. 6—9, from preliminary probability plots, and from the massive literature pertaining to particle-size distributions in sediments and sedimentary rocks. The principal conclusion from the cumulative probability curves is that they plot as two, usually three, or sometimes four straight line segments which are connected by a jog or lazy S-shaped connection. This appearance of the plots clearly reflects the multimodal nature of the gouge samples, which, in turn, reflects the presence of fine-, medium, and coarse-grained subpopulations. Multimodal situations normally arise from mixed populations of more than one source of variation.

Petrochemistry

The objective of this phase of research was to determine the extent of chemical leaching and/or enrichment (including hydration) that occurs in the process of gouge formation. In addition, petrochemical data, combined with mineralogic data, allows one to evaluate whether the development of gouge is an *in situ* process or to some extent involves mixing of materials juxtaposed by fault movement.

Analytical data are presented in Tables IV—VI. For this work, Site 4, the core into a tonalite pluton near Lake Hughes, was ideal for its relative homogeneity minimized its natural compositional variations so that changes with respect to alteration and/or gouge development could be ascertained. Much of the compositional variation that can be noted in Table VI is due to minor fractional crystallization which is discussed below. Hydration appears to be the only chemical change that is common to all gouge samples. However, the amount of hydration is surprisingly small as gouge samples have only 1.70—4.75 wt.% volatiles compared to 0.47—1.46 wt.% for the parent rock. The main volatile component is H_2O and the average amount of hydration with cataclasis was only 2.19%.

To see through the hydration, the sample analyses were recalculated on a

TABLE IV

Whole rock analyses [a] of gouge from Big Pines (Site 2) and Painted Canyon (Site 1)

	BP-1	BP-2	BP-3	BP-4	BP-5	PC-1	PC-2	PC-3	PC-4
SiO_2 [b]	56.61	68.57	58.53	60.81	72.25	65.07	61.57	60.65	61.01
TiO_2	0.85	0.13	0.92	0.79	0.49	0.47	0.77	0.73	1.15
Al_2O_3	15.96	13.49	16.67	15.02	12.29	13.75	13.14	11.62	13.67
FeO [c]	5.74	0.85	5.62	4.56	2.96	5.41	7.66	6.13	8.78
MgO	3.75	0.29	3.45	2.87	1.44	2.47	3.83	4.15	4.09
MnO	0.119	0.014	0.124	0.068	0.034	0.106	0.172	0.149	0.165
CaO	6.46	4.25	5.66	4.72	2.32	2.90	4.42	6.28	2.46
Na_2O	3.26	2.76	3.48	2.26	2.04	3.33	2.16	2.80	1.78
K_2O	2.56	6.56	2.26	2.84	3.34	2.16	1.55	1.16	2.12
L.O.I. [d]	3.36	3.38	2.27	4.82	3.19	2.93	3.47	5.59	3.74
Total	98.66	100.29	98.99	98.76	100.36	98.59	98.74	99.26	98.97
Li	37.4	16.7	31.7	32.4	27.5	29.1	38.7	42.7	42.5
Rb	94.4	188	104	113	154	67.6	74.1	38.2	93.2
Sr	426	362	612	680	204	301	270	327	162
Ba	740	1828	781	1134	766	1067	313	422	543

[a] Analyses completed at U.S.C. Petrochemistry Laboratory by Gregory Benson and J. Lawford Anderson.

[b] Major elements as wt.% oxide; Li, Rb, Sr, Ba as ppm.

[c] All Fe as FeO.

[d] Loss on ignition: volatile loss at 1000°C, includes $H_2O + CO_2$.

TABLE V

Whole rock analyses [a] of gouge from Tejon pass-Site 3

	TP-1	TP-2	TP-3	TP-6a	TP-6b	TP-6c	TP-7	TP-8
SiO_2 [b]	60.03	50.31	72.67	59.58	58.64	56.91	57.17	64.08
TiO_2	1.29	1.44	0.085	0.74	1.04	1.39	0.97	0.791
Al_2O_3	16.69	18.05	14.25	16.42	16.32	17.55	16.43	15.91
FeO [c]	5.22	7.36	0.671	4.36	5.72	6.21	5.35	3.96
MgO	2.30	4.15	0.120	1.84	2.77	2.95	2.39	1.85
MnO	0.077	0.108	0.032	0.071	0.086	0.089	0.066	0.071
CaO	4.18	6.02	0.791	3.34	4.55	5.30	5.12	3.45
Na_2O	5.21	3.95	4.06	5.11	4.83	5.10	4.03	3.78
K_2O	1.54	1.79	5.60	2.28	1.68	0.927	1.79	2.85
L.O.I. [d]	2.53	4.80	0.85	3.27	3.82	3.66	4.14	3.67
Total	99.07	97.98	99.13	97.02	99.46	100.09	97.46	100.41
Rb2	49.6	69.7	156	74.2	58.4	28.0	59.2	80.8
Sr	507	466	211	537	518	573	495	377
Ba	833	469	817	905	755	372	1014	1137

[a] Analyses completed at U.S.C. Petrochemistry Laboratory by Gregory Benson and J. Lawford Anderson.

[b] Major elements at wt.% oxide; Rb, Sr, Ba, as ppm.

[c] All Fe as FeO.

[d] Loss of ignition, volatile loss at 1000°C; includes $H_2O + CO_2$.

TABLE VI

Whole rock analyses [a] of tonalite and derived gouge from Site 4

	2-11	2-12	2-13A	2-13B	2-27	2-33	2-41	2-46	2-51A	2-52B	2-52C	2-53B	2-54A
SiO_2 [b]	64.43	66.82	63.00	62.98	63.75	63.79	62.01	63.98	62.41	63.55	58.95	61.20	61.62
TiO_2	0.82	0.78	0.76	0.69	0.95	0.85	0.85	0.86	0.78	0.81	0.88	0.87	0.87
Al_2O_3	17.53	15.13	16.63	15.86	16.64	17.36	16.04	17.05	17.17	16.95	16.85	16.51	16.84
FeO [c]	3.83	3.99	4.00	3.73	4.27	4.22	3.95	4.03	4.29	3.81	3.92	4.12	4.01
MgO	1.59	1.59	1.24	1.82	2.07	1.67	2.49	1.18	1.77	1.48	1.59	1.47	1.46
MnO	0.055	0.051	0.065	0.068	0.071	0.066	0.073	0.058	0.061	0.063	0.064	0.058	0.066
CaO	4.98	3.31	4.97	3.79	3.40	4.68	5.08	5.07	4.20	3.53	6.32	4.42	5.04
Na_2O	4.19	3.67	4.19	4.09	3.25	4.08	4.26	4.25	4.29	4.82	3.82	4.45	4.18
K_2O	2.10	3.83	1.90	2.78	3.35	2.38	2.19	2.02	2.36	2.41	1.88	2.15	2.42
L.O.I. [d]	0.47	1.70	1.10	3.17	1.90	0.80	1.06	1.49	nd [e]	nd	4.75	3.91	3.56
Total	100.00	100.87	97.86	98.99	99.65	99.90	98.00	99.99	—	—	99.02	99.16	100.07
Li	37.7	40.1	38.4	33.8	39.3	38.9	41.7	44.1	38.3	33.0	36.1	33.1	36.9
Rb	86.3	170	104	125	126	99.6	113	111	126	114	79.9	89.1	105
Sr	877	602	798	640	773	832	847	794	829	883	598	558	870
Ba	811	1224	448	717	1324	844	659	534	543	588	457	481	587

[a] Analyses completed at U.S.C. Petrochemistry Laboratory by Sona Stapleford, Gregory Benson, and J. Lawford Anderson.
[b] Major elements as wt.% oxide; Li, Rb, Sr, and Ba as ppm.
[c] All Fe and FeO.
[d] Loss of ignition, volatile loss at 1000°C, includes $H_2O + CO_2$.
[e] nd = no data.

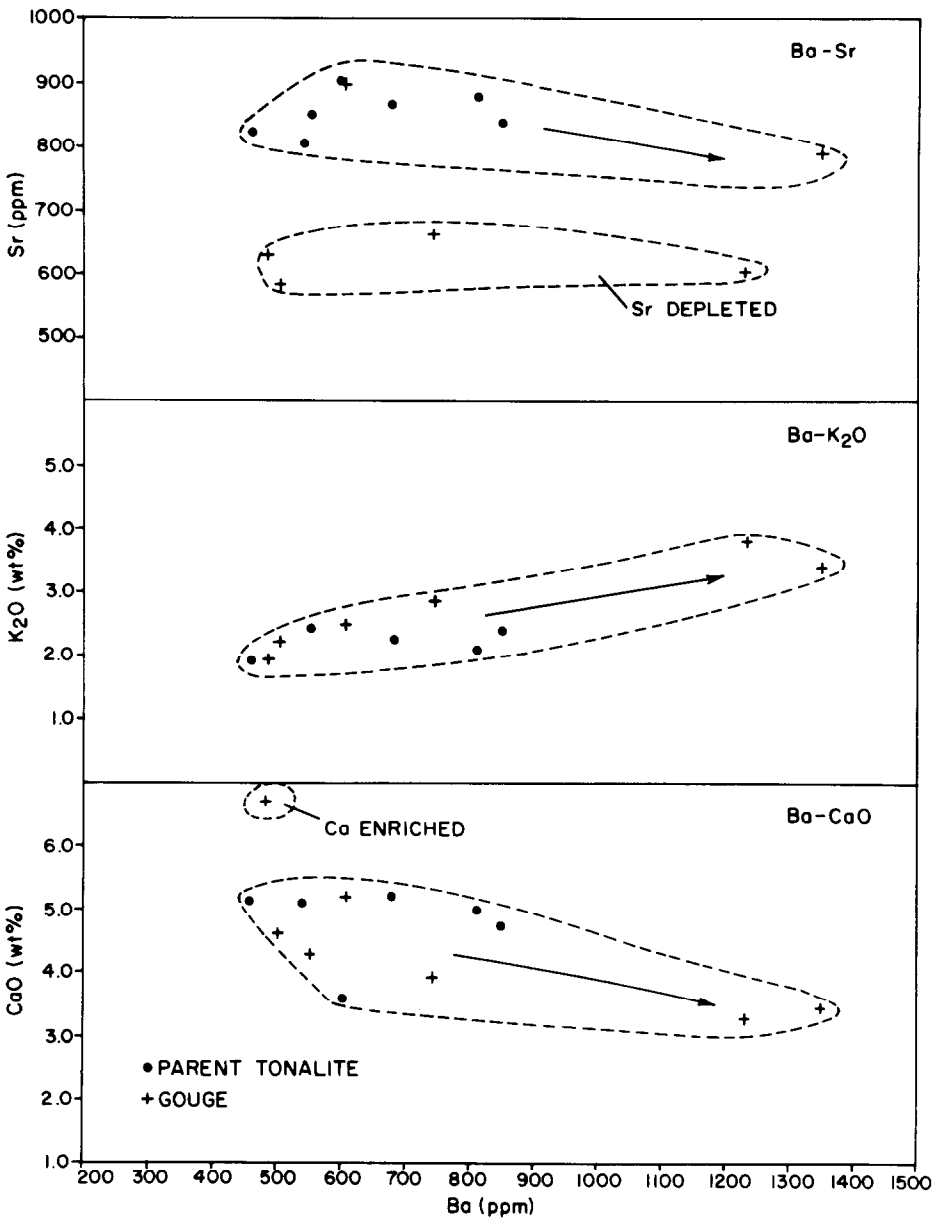

Fig. 10. Selected compositional data for tonalite and derived gouge from Site 4.

volatile-free basis and some these data are presented in Fig. 10. For the total core, there is a major increase in Ba from 463 to 1354 ppm with a parallel increase in K_2O (1.96—3.86%) and decrease in Sr and CaO. This is a typical trend expected from plagioclase-dominated fractionation in a tonalitic mag-

ma. Figure 10 provides a basis to evaluate the extent of disturbance of these primary petrochemical trends by the cataclasis. The arrows in this figure depict the trend with increasing fractionation and it is evident that no disturbance occurs for Ba and K_2O. Yet from the Ba—Sr plot, it is evident that four of the six gouge samples show a depletion in Sr and from the Ba—CaO plot, one of the six gouge samples has an enrichment in Ca. The latter sample is 2.52C which, from its modal analysis, also shows an anomalously high calcite percentage. In summary, the Lake Hughes core shows that gouge formation was essentially an *in situ*, isochemical process. Hydration occurs in all gouge samples but the amount of hydration is minimal. With the exception of Ca and Sr, the compositional constituents Si, Al, Fe, Mg, Mn, Na, K, Li, Rb, and Ba exhibit no change due to the cataclasis.

Data from Tejon pass further support these conclusions. The samples TP-6a, TP-6b, and TP-6c were collected within a quartz diorite-tonalite fault block to document changes that occur with increasing gouge development. The three samples were all collected within a meter of each other and although they exhibit a range of chemistry, there is no change that can be attributed to cataclasis. Observed compositional changes (increasing Ca, Fe, Mg, Ti and Ba with decreasing Si, K, Rb) are again those one would predict for dioritic melts. The fact that such delicate pre-fault (magmatic) compositional trends are so well preserved within a gouge zone is further testimony to the lack of chemical mobility.

Samples from Big Pines and Painted Canyon do not provide as good a basis to ascertain chemical mobility during cataclasis since all samples have been totally transformed into gouge. However, the major and trace element compositions are typical for these kinds of igneous rocks. No significant changes in composition due to cataclasis are observed. Again, the amount of hydration in these samples is small (maximum volatile content is 5.59%). Indeed gouge developed from granite pegmatite, which of these samples contains the least amount of hydrous silicates (Sample TP-3, Table V), also has the lowest volatile content (0.85 wt.%).

SUMMARY

Expectedly, unindurated gouge typifies the cataclastic rocks generated at the near surface levels of the San Andreas fault. However, the nature of gouge derived from the predominately igneous terrane transected by the fault in southern California differs from the "clay-gouge" reported by Wu et al. (1975) and Wu (1977) for central California.

Clay development in the gouge is minimal and is of the kaolinite variety with montmorillonitic and illitic clays being absent. This gouge, which is derived from igneous dioritic to granitic parent rocks, is essentially a rock flour with a mineralogy representing the milled-down equivalent of the original rock. The gouge mineralogy is determined to a large extent by the mineralogy of the associated protolith. Major alterations involve oxidation, some

hydration of ferromagnesian silicates, and the introduction of calcite. It is clear that some minerals (chlorite and calcite) continue to form, be reformed or be introduced during gouge development. Many of the other alterations are likely due to late stage deuteric alterations unrelated to faulting. Low temperature secondary minerals are rare. Although abundant clay and perhaps zeolite facies minerals were expected to occur within the gouge zone, they were not found. In general, the gouge minerals did not reequilibrate with the imposed P-T regime during cataclasis and are relict from an earlier igneous or metamorphic history. In thin section, it is evident that the minerals forming the gouge matrix are derived from nearby large grains.

Texturally, the rocks are dominated by fine sand- to silt-size particles. The amount of clay-size material is low but there is a general decrease in particle size with depth and increasing confining pressure with the predominant mode shifting sequentially from sand- to silt-size material. The grain-size distribution is also polymodal. Grain surface microtextures include fracture and breakage surfaces, etching, and smooth undulatory topography. Petrochemically, the development of this type of gouge is largely an isochemical process. A small amount of hydration occurs in all gouge samples but is of minimal importance. Some changes occurred for Sr and Ca during cataclasis but not in all samples and as for Si, Al, Ti, Fe, Mg, Mn, K, Na, Li, Rb, and Ba, no leaching and/or enrichment occurred.

Gouge development in these igneous terrances appears to be largely an *in situ* process with direct dependence on the host rock. Mixing of rock types is apparently insignificant and the original textural and compositional integrity of these rocks is often not obliterated. Fabric analyses indicates that brecciation (shattering), not shearing, is the major mechanism at these upper crustal levels.

We are presently investigating cataclastic rocks within the San Gabriel fault which, as a deeply eroded precursor to the San Andreas, may provide intrafault material more representative of deeper crustal levels.

ACKNOWLEDGEMENTS

This research has been supported by a grant (Grant No. 14-08-0001-G484) from the Office of Earthquake Studies, U.S. Geological Survey. We are indebted to a number of workers who aided us in the technical aspects of the study, specifically: Emmanuel Perez — X-ray analyses; Stephanie McCoul — modal analyses, Gregory A. Benson, Sona Stapleford, and Whitney A. Moore — whole rock chemistry; Paul M. Adams — electron microprobe analyses; Marilyn Logan, Jeff Werter, and Christine Farrens — textural analyses; and Dave Smith — scanning electron microscopy. We also wish to thank Professor Thomas L. Henyey for providing access to core LH-2 (Site 4).

REFERENCES

Albee, A.L. and Ray, L., 1970. Correction factors for electron probe microanalysis of silicates, oxides, carbonates, phosphates, and sulfates. Anal. Chem., 42: 1408—1414.

Aydin, 1977. Small faults formed as deformation bands in sandstone. U.S.G.S., Proc Conf. II, Experimental Studies of Rock Friction with Application to Earthquake Prediction, pp. 617—653.

Bence, A.E. and Albee, A.L., 1968. Empiracle correction factors for the electron microanalysis of silicates and oxides. Geol., 76: 382—403.

Brace, W.F., 1972. Laboratory studies of stick-slip and their application to earthquakes. Tectonophysics, 14: 189—200.

Byerlee, J., Mjachkin, V., Summers, R. and Voevoda, O., 1978. Structures developed in fault gouge during stable sliding and stick-slip. Tectonophysics, 44: 161—171.

Carver, R.E. (Editor), 1971. Procedures in Sedimentary Petrology. Wiley-Interscience, New York, N.Y., 458 pp.

Engelder, J.T., 1974. Cataclasis and the generation of fault gouge. Geol. Soc. Am. Bull., 85: 1515—1522.

Higgins, M.W., 1971. Cataclastic rocks. U.S.G.S. Profess. Pap., 687: 97 pp.

Krinsley, D. and Smalley, I., 1973. Shape and nature of small sedimentary quartz particles. Science, 180: 1277—1279.

Logan, J.M., 1977. Creep, stable sliding, and premonitory slip. U.S.G.S., Proc. Conf. II, Experimental Studies of Rock Friction with Application to Earthquake Prediction, pp. 205—237.

Logan, J.M., 1978a. Laboratory and field investigations of fault gouge In: J.F. Evernden (Editor), Summaries of Technical Reports, 6. U.S. Geological Survey, Washington, D.C., pp. 370—373.

Logan, J.M., 1978b. Laboratory and field investigations of fault gouge. In: J.F. Evernden (Editor), Summaries of Technical Reports, 7. U.S. Geological Survey, Washington, D.C., pp. 492—494.

Margolis, S.V. and Krinsley, D.H., 1974. Processes of formation and environmental occurrence of microfeatures on detrital quartz grains. Am. J. Sci., 274: 449—464.

Miller, W.J., 1944. Geology of the Palm Springs Blythe strip, Riverside Co., California. Calif. J. Mines Geol., 40: 11—72.

Nason, R.D., 1972. Propagation of fault creep events. NOAA Tech. Rep., ERL 236-ESL, 21 pp.

Nason, R.D., 1973. Fault creep and earthquakes on the San Andreas fault. In: R.L. Kovach and A. Nur (Editors), Proceedings of the Conference on Tectonic Problems of the San Andreas Fault System. Stanford Univ. Press Publ., 13: 275—285.

Pettijohn, F.J., 1975. Sedimentary Rocks. Harper and Row, New York, N.Y., 628 pp.

Scholz, C., P. Molnar and T.L. Johnson, 1972. Detailed studies of frictional sliding of granite and implications for the earthquake mechanism. J. Geophys. Res., 77: 6392—6406.

Stesky, R.M. and W.F. Brace, 1973. Estimation of frictional stress on the San Andreas fault from laboratory measurements. In: R.L. Kovach and A. Nur (Editors), Proceedings of the Conference on Tectonic Problems of the San Andreas Fault System. Stanford Univ. Press Publ., 13: 206—214.

Sylvester, A.G. and R.R. Smith, 1975. Structure section across the San Andreas fault zone, Mecca Hills. Calif. Div. Geol. Spec. Rep., 118: 111—118.

Wang, C.Y., 1977. Experimental investigation of mechanical properties of clay gouge and cataclastics along the San Andreas fault. In: J.F. Evernden (Editor), Summary of Technical Reports, 3. U.S. Geological Survey, Office of Earthquake Studies, pp. 28—34.

Wu, F.T., L. Blatter and H. Robertson, 1975. Clay gouges in the San Andreas fault system and their possible implications. Pure Appl. Geophys., 113: 87—95.

Wu, F.T., 1977. Mineralogy and physical nature of clay gouge. U.S.G.S., Proc. Conf. II, Experimental Studies of Rock Friction with Application to Earthquake Prediction, pp. 389—445.